PHYSICAL REVIEW E **83**, 030302(R) (2011)

Critical scaling of shearing rheology at the jamming transition of soft-core frictionless disks

Peter Olsson[1] and S. Teitel[2]
[1]*Department of Physics, Umeå University, S-901 87 Umeå, Sweden*
[2]*Department of Physics and Astronomy, University of Rochester, Rochester, New York 14627, USA*
(Received 28 October 2010; published 17 March 2011)

We perform numerical simulations to determine the shear stress and pressure of steady-state shear flow in a soft-disk model in two dimensions at zero temperature in the vicinity of the jamming transition ϕ_J. We use critical point scaling analyses to determine the critical behavior at jamming, and we find that it is crucial to include corrections to scaling for a reliable analysis. We find that the relative size of these corrections are much smaller for pressure than for shear stress. We furthermore find a superlinear behavior for pressure and shear stress above ϕ_J, both from the scaling analysis and from a direct analysis of pressure data extrapolated to the limit of vanishing shear rate.

DOI: 10.1103/PhysRevE.83.030302 PACS number(s): 45.70.−n, 64.60.−i

Granular materials, supercooled liquids, and foams are examples of systems that may undergo a transition from a liquid-like to an amorphous solid state as some control parameter is varied. It has been hypothesized that the transitions in these strikingly different systems are controlled by the same mechanism [1], and the term jamming has been coined for this transition.

Much work on jamming has focused on a particularly simple model, consisting of frictionless spherical particles with repulsive contact interactions at zero temperature [2]. The packing fraction (density) of particles ϕ is the key control parameter in such systems. Jamming upon compression and jamming by relaxation from initially random states have been the focus of many investigations [2–4]. Another physically realizable and important case is jamming upon shear deformation. This has been modeled both by simulations at a finite constant shear strain rate $\dot\gamma$ [5–11] as well as by quasistatic shearing [4,12,13], in which the system relaxes to its energy minimum after each finite small strain increment.

Several attempts have been made to determine the critical packing fraction ϕ_J and critical exponents that describe behavior at shear-driven jamming [5–8,10,11]. There is, however, little agreement on the values of the exponents and there is thus a need for a thorough and careful investigation of the jamming transition in the shearing ensemble. It will also be interesting to compare the exponents found from shearing rheology to those found from compressing marginally jammed packings. In particular, we note the linear increase of pressure above jamming that is observed in that system [2,3], compared to the superlinear behavior often reported in the sheared system for pressure and/or shear stress [5,6,10,11].

In this paper we do a careful scaling analysis of high-precision data for both shear stress and pressure at shear strain rates down to $\dot\gamma = 10^{-8}$. Instead of relying on visually acceptable data collapses we use a nonlinear minimization technique to determine the best fitting parameters. As in a recent analysis of energy-minimized configurations [4] we find that it is necessary to include corrections to scaling, but also that the magnitude of the corrections are markedly different for different quantities and, furthermore, that the neglect of these corrections is a major reason for the differing values of the critical exponents in the literature. We find strong evidence for a superlinear behavior of yield stress and pressure above jamming from the scaling analysis and also find independent support for this result from pressure data extrapolated to the limit of vanishing shear rate. We also suggest a possible mechanism behind this behavior.

Following O'Hern *et al.* [2] we use a simple model of bi-disperse frictionless soft disks in two dimensions with equal numbers of disks with two different radii in the ratio 1.4. Length is measured in units of the diameter of the small particles, d_s. With r_{ij} being the distance between the centers of two particles and d_{ij} being the sum of their radii, the interaction between overlapping particles is $V(r_{ij}) = (\epsilon/2)(1 - r_{ij}/d_{ij})^2$. We use Lees-Edwards boundary conditions [14] to introduce a time-dependent shear strain $\gamma = t\dot\gamma$. With periodic boundary conditions on the coordinates x_i and y_i in an $L \times L$ system, the position of particle i in a box with strain γ is defined as $\mathbf{r}_i = (x_i + \gamma y_i, y_i)$. We simulate overdamped dynamics at zero temperature with the equation of motion [15]

$$\frac{d\mathbf{r}_i}{dt} = -C \sum_j \frac{dV(\mathbf{r}_{ij})}{d\mathbf{r}_i} + y_i \dot\gamma \hat{x},$$

with $\epsilon = 1$ and $C = 1$. The unit of time is $\tau_0 = d_s/(C\epsilon)$.

Our basic scaling assumption describes how different quantities (e.g., shear stress, pressure, potential energy, and jamming fraction) depend on a change of length scale with a scale factor b:

$$\mathcal{O}(\delta\phi, \dot\gamma, 1/L) = b^{-y_\mathcal{O}/\nu} g_\mathcal{O}(\delta\phi b^{1/\nu}, \dot\gamma b^z, b/L). \qquad (1)$$

Here $\delta\phi = \phi - \phi_J$, $y_\mathcal{O}$ is the critical exponent of the observable $\mathcal{O}$, ν is the correlation length exponent, and z is the dynamic critical exponent. Point J is at $\delta\phi = 0, \dot\gamma \to 0$, and an infinite system size, $1/L \to 0$. The scaling relation describes the departure from the critical point in these respective directions.

The above expression is the starting point for our analysis. Just as in Ref. [5] we make use of data obtained at finite shear rates and system sizes large enough that finite-size effects may be neglected: $N \geqslant 65\,536$ at the lower shear rates. With $b = \dot\gamma^{-1/z}$ in Eq. (1) and $q_\mathcal{O} \equiv y_\mathcal{O}/z\nu$, the scaling relation becomes

$$\mathcal{O}(\delta\phi, \dot\gamma) \sim \dot\gamma^{q_\mathcal{O}} g_\mathcal{O}(\delta\phi/\dot\gamma^{1/z\nu}), \qquad (2)$$

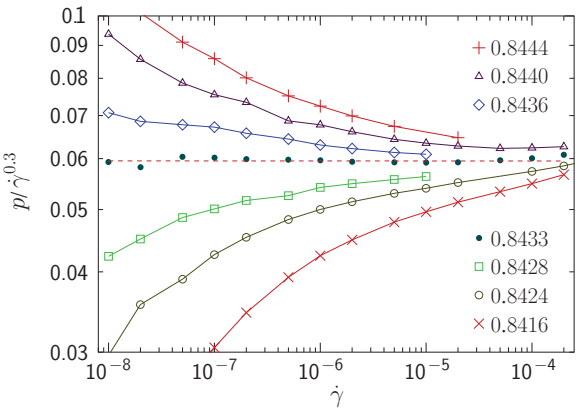

FIG. 1. (Color online) Approximate determination of ϕ_J and q_p from Eq. (2) without corrections to scaling. The figure shows pressure versus shear rate at several different packing fractions. The pressure is shown as $p/\dot{\gamma}^{0.3}$ to make the behavior clearly visible. This suggests that $p \sim \dot{\gamma}^{q_1}$ with $q_1 = 0.30$ at $\phi_{J1} = 0.8433$.

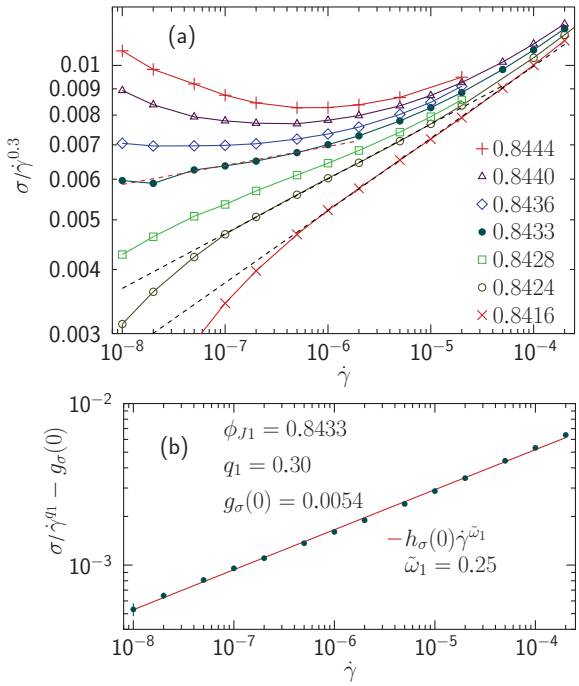

FIG. 2. (Color online) Shear stress σ versus shear rate $\dot{\gamma}$ at several different densities. Panel (a) shows that there is no density where σ behaves algebraically across the extended range of shear rates; however, data across two orders of magnitude of $\dot{\gamma}$ could, to a reasonable approximation, be taken as algebraic. In that vein, data limited to $\dot{\gamma} \geqslant 10^{-6}$ give $\phi = 0.8416$ (crosses) as a good candidate for ϕ_J (cf. Ref. [5]), whereas other ranges of $\dot{\gamma}$ would give other estimates. From a comparison with $p/\dot{\gamma}^{q_1} = g_p(0)$ at $\phi = \phi_{J1}$ in Fig. 1, panel (b) shows the correction term $\sigma/\dot{\gamma}^{q_1} - g_\sigma(0)$ at ϕ_{J1}, and it appears that this correction is, to a very good approximation, $\sim\dot{\gamma}^{\tilde{\omega}_1}$, which has the same form as standard corrections to scaling in critical phenomena.

where the scaling function is a function of only a single argument. At ϕ_J we have $\mathcal{O}(\phi_J, \dot{\gamma}) \sim \dot{\gamma}^{q_\mathcal{O}}$, which gives a simple method for determining $q_\mathcal{O}$ and ϕ_J: Plot $\mathcal{O}$ versus $\dot{\gamma}$ on a double-log scale for several different ϕ. The packing fraction for which the data fall on a straight line is then our estimated ϕ_J. Data above and below ϕ_J, respectively, should curve in opposite directions.

We start by applying this simple recipe to the pressure p and will turn to the shear stress only at the next step. Both these quantities are calculated, as in Ref. [2], from the elastic forces only. Figure 1 shows pressure versus shear rate at several different packing fractions. Anticipating that the value of $q_p \approx 0.3$, we plot $p/\dot{\gamma}^{0.3}$ versus $\dot{\gamma}$ in order to more clearly differentiate the behaviors near ϕ_J. It is then easy to identify $\phi_{J1} = 0.8433$ as the density with a rectilinear behavior, at which we find $p \sim \dot{\gamma}^{q_1}$ with $q_1 = 0.3$. Data at lower and higher densities curve downward and upward, respectively. The values ϕ_{J1} and q_1 are only first estimates of the jamming density and exponent, respectively; our final estimates turn out to be just slightly different.

Figure 2 is the same kind of plot for the shear stress σ, and it is immediately clear that these data are not directly amenable to the same kind of analysis; there is no density with an algebraic behavior across the whole range of shear rates. Before presenting our further analyses we note that this provides an explanation for the differing values of both jamming density and exponents in the literature. In Ref. [5] the jamming density was found to be $\approx$0.8415 and the figure shows that data in the range $10^{-6} \leqslant \dot{\gamma} \leqslant 10^{-4}$ would suggest $\phi = 0.8416$ (crosses) as a good candidate for ϕ_J. However, it is clear that data at the same density and lower shear rates deviate from the algebraic behavior. Similarly, with access to σ down to $\dot{\gamma} = 10^{-7}$, $\phi = 0.8424$ (open circles) would appear as a good candidate for ϕ_J, whereas data in the range $10^{-8} \leqslant \dot{\gamma} \leqslant 10^{-6}$ would suggest $\phi_J = 0.8433$ (solid dots). The value of the effective exponent q_σ also changes: For these three different ranges of shear rates we find $q_\sigma = 0.44$, 0.41, and 0.33, respectively. Note that this explanation is at variance with Ref. [11] where the differing exponents are attributed to using data from an excessively large range in ϕ. That explanation is not applicable here since our analyses only consider data right at the presumed ϕ_J.

The inconsistencies suggested by Fig. 2 can be resolved by realizing that corrections to scaling [16] must be considered. Corrections to scaling, arising from the leading irrelevant variable in a renormalization group picture, require that Eq. (1) be modified by an additional term:

$$\mathcal{O}(\delta\phi, \dot{\gamma})/b^{-y_\mathcal{O}/\nu} = g_\mathcal{O}(\delta\phi b^{1/\nu}, \dot{\gamma} b^z) + b^{-\omega} h_\mathcal{O}(\delta\phi b^{1/\nu}, \dot{\gamma} b^z),$$

where $h_\mathcal{O}$ is another scaling function and ω is the correction-to-scaling exponent. Using $b = \dot{\gamma}^{-1/z}$ in the above then gives

$$\mathcal{O}(\delta\phi, \dot{\gamma})/\dot{\gamma}^{q_\mathcal{O}} = g_\mathcal{O}(\delta\phi/\dot{\gamma}^{1/z\nu}) + \dot{\gamma}^{\omega/z} h_\mathcal{O}(\delta\phi/\dot{\gamma}^{1/z\nu}). \quad (3)$$

For the shear stress at ϕ_J (i.e., $\delta\phi = 0$), this simplifies to

$$\sigma(0, \dot{\gamma})/\dot{\gamma}^{q_\sigma} = g_\sigma(0) + \dot{\gamma}^{\omega/z} h_\sigma(0). \quad (4)$$

If we take $\phi_J = \phi_{J1}$ and $q_\sigma = q_1 = 0.3$ from the analysis of the pressure in Fig. 1, then the deviations of the stress from the simpler scaling assumption, $\sigma(\phi_J, \dot{\gamma})/\dot{\gamma}^{q_1} = g_\sigma(0)$, can be shown to precisely obey the form of Eq. (4). From Fig. 2(a) we note that $\sigma/\dot{\gamma}^{q_1}$ in the limit of low $\dot{\gamma}$ appears to saturate at a finite value, $0.005 < g_\sigma(0) < 0.006$, and so we plot $\sigma/\dot{\gamma}^{q_1} - g_\sigma(0)$ in Fig. 2(b). It is then possible to adjust $g_\sigma(0)$ such that

the remainder is algebraic in $\dot\gamma$, and Eq. (4) is fulfilled with $\omega/z = \tilde\omega_1 \approx 0.25$.

The above analysis of σ relied on ϕ_{JI} and q_1 determined from the pressure data without corrections to scaling. We now set out to analyze both pressure and shear stress directly from the scaling relation Eq. (3) that includes the correction term and determine the ϕ_J, $q_{\mathcal{O}}$, $1/z\nu$, and ω/z that allow for the best fit to Eq. (3). Here $g_{\mathcal{O}}$ and $h_{\mathcal{O}}$ are scaling functions, which we approximate with fifth-order polynomials in $x \equiv \delta\phi/\dot\gamma^{1/z\nu}$. The actual fits are done by minimizing χ^2/DOF (where DOF is the degrees of freedom) with a Levenberg-Marquardt method. The number of points in the fits range from about 100 to 250 depending on the range of data used in the fits.

In this kind of involved analysis it is crucial to validate the results and, to that end, we use several different criteria: (i) The first is to check the quality of the fits. Are the deviations of the data from the scaling function consistent with the statistical uncertainties? We use χ^2/DOF, which should be close to unity, to get a quantitative measure. (ii) A good quality of fit does, however, not by itself guarantee that the results are reliable. The second check is therefore whether the fitting parameters are reasonably independent of the precise range of the data included in the fit. We do this by systematically varying both the range of shear rates and the range of densities; fixing $X = (\phi - 0.8434)/\dot\gamma^{0.26}$ we use the criterion $|X| < X_{\max}$ with $X_{\max} = 0.2$, 0.3, and 0.4. This restriction does not reflect the size of the critical region but rather that the polynomial approximation of the scaling function breaks down for excessively large X. (iii) A final check is whether the critical parameters from analyses of different quantities (here p and σ) agree with one another.

Figure 3 shows χ^2/DOF and the key fitting parameters ϕ_J, $1/z\nu$, q_p, and q_σ plotted against $\dot\gamma_{\max}$. For each quantity the left and right panels are from analyses of pressure and shear stress, respectively. First considering χ^2/DOF in the first pair of panels, we note that the fits are only good when the data are taken from a rather restrictive interval in ϕ around ϕ_J, $|X| \leqslant 0.3$. For pressure there is a good fit to the data over a very large interval—more than four decades in $\dot\gamma$. For the shear stress the highest shear rates should not be used, and reliable results are obtained by restricting $\dot\gamma$ to $\dot\gamma \leqslant 5 \times 10^{-5}$ when $X_{\max} = 0.2$ and $\dot\gamma \leqslant 1 \times 10^{-5}$ for $X_{\max} = 0.3$.

The next two panels show ϕ_J from pressure and shear stress, respectively, in good agreement with one another; we estimate $\phi_J = 0.843\,47 \pm 0.000\,20$, in agreement with other recent determinations of ϕ_J from quasistatic simulations [4,12]. Here and throughout, the error bars in the figures are one standard deviation whereas the numerical values give a min-max interval ($\pm$ three standard deviations) for the estimated quantities. To correctly interpret these figures one should note that the fitted values for different $\dot\gamma_{\max}$ and $X_{\max}$ are based on different subsets of the same data, and therefore are expected to be strongly correlated. The main point is here to check how robust the fitting parameters are to changes in the precise data set, and the absence of clear trends in the results is therefore an encouraging sign.

We further find $1/z\nu = 0.26 \pm 0.02$ and $q = 0.28 \pm 0.02$. Combining the two exponents we find $y = qz\nu = 1.08 \pm 0.03$ (a strong correlation between q and $1/z\nu$ is responsible for the error estimate for y). Since y is just slightly above unity we have also reanalyzed the pressure data with the assumption $y_p = 1$. The fits then become considerably worse and we conclude that the data are strongly in favor of $y_p > 1$. A similar analysis of the shear stress is not conclusive. Using $\nu = 1.09$ from Ref. [4] the dynamic critical exponent becomes $z = 3.5 \pm 0.4$. The correction-to-scaling exponent (not shown) is $\omega/z = 0.29 \pm 0.03$, or $\omega\nu = 1.10 \pm 0.06$, which, again using $\nu = 1.09$ [4], gives $\omega = 1.0 \pm 0.1$, in good agreement with Ref. [4].

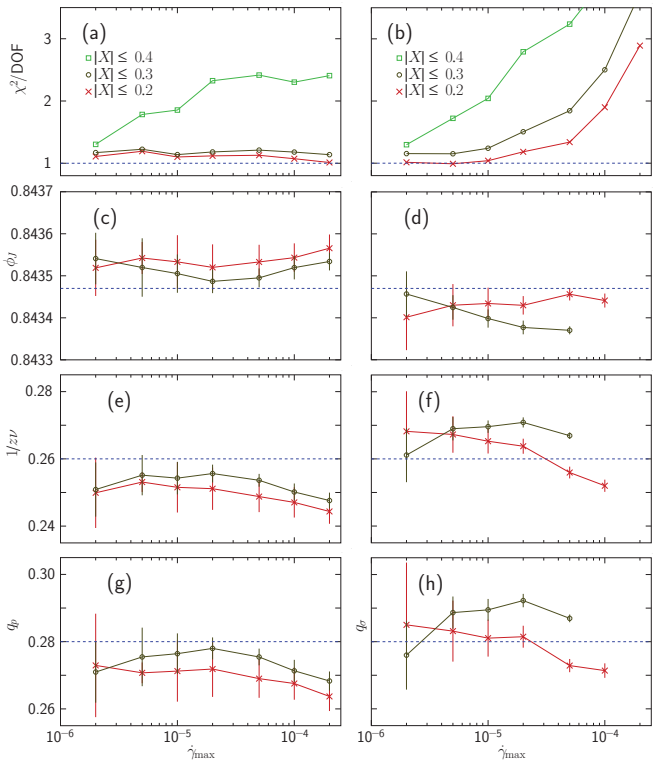

FIG. 3. (Color online) Results from scaling analyses that include corrections to scaling. The left and right panels are from analyses of pressure and shear stress, respectively. The first pair of panels, which give χ^2/DOF, suggest that the analyses are only reliable when data is used in a rather restrictive interval of $\phi - \phi_J$, $|X| \leqslant 0.3$. For shear stress one also has to be restrictive in using data with larger $\dot\gamma$. From the following panels we read off $\phi_J = 0.843\,47$, $1/z\nu = 0.26$, and $q_p = q_\sigma = 0.28$. Combining the last two ($y = qz\nu$) gives $y_p = y_\sigma = 1.08$.

With these more complicated analyses it is no longer possible to determine ϕ_J directly from a simple plot as in Fig. 1. The most direct way to illustrate the determination of ϕ_J is shown in Fig. 4 which displays $p/\dot\gamma^{q_p}$ and $\sigma/\dot\gamma^{q_\sigma}$ against $\dot\gamma^{\omega/z}$, now with linear scales on both axes. Data at ϕ_J should then fall on a straight line. Note the very different size of the corrections, given by the slopes of the data.

For ϕ well above ϕ_J the pressure decays algebraically in $\dot\gamma$ and this gives a means to determine the limiting value $p(\phi, \dot\gamma \to 0)$. If we can get reliable values, $p(\phi, \dot\gamma \to 0)$, at densities sufficiently close above ϕ_J it should be possible to get another determination of y_p, independent of the scaling analysis. Figure 5 shows some of our finite-$\dot\gamma$ data together with such extrapolated values for densities down to $\phi = 0.848$.

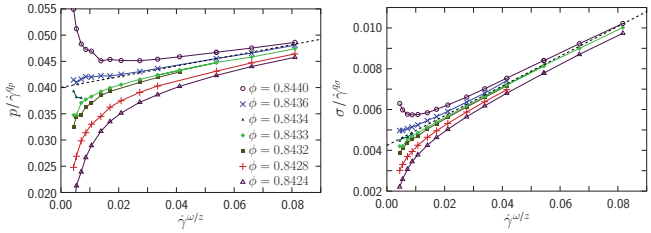

FIG. 4. (Color online) Illustration of results of the scaling analysis. The dashed lines are the behaviors at ϕ_J for p and σ, respectively: $\mathcal{O}(\phi_J,\dot\gamma)/\dot\gamma^{q_\mathcal{O}} = g_\mathcal{O}(0) + \dot\gamma^{\omega/z} h_\mathcal{O}(0)$.

Fitting to the five points from $\phi = 0.848$ through 0.856 (0.5% through 1.5% above ϕ_J) we find $y = 1.09 \pm 0.04$ shown by the solid line, in excellent agreement with $y = 1.08$ from the scaling analysis. (The inset of Fig. 5 shows how y depends on the assumed ϕ_J.) Similar results, $y_p \approx 1.1$, have also been found before [13,17].

The above results point to a good agreement between the exponent obtained from the scaling analyses on the one hand, and the $\dot\gamma \to 0$ limit of the pressure above ϕ_J on the other, which is entirely in accordance with expectations from critical scaling. This is in contrast to the claim in Ref. [11] that the critical region is extremely narrow and does not include densities away from ϕ_J in the limit $\dot\gamma \to 0$; the yield stress is there taken to be governed by a different regime with a different exponent, $y_\sigma = 3/2$.

With the result $y \approx 1.1$ from two different analyses it becomes important to try and reconcile this with the well-established linear increase of the pressure when marginally jammed packings are compressed above their respective jamming densities [2,3]. We speculate that the reason for this is that the ensemble of configurations depends in a nontrivial way on ϕ in the vicinity of ϕ_J, and that this is so since the dynamic process that generates this ensemble is itself very sensitive to ϕ. It is then relevant to consider the behavior in the quasistatic limit and to recall that the average time needed for the minimization of energy in quasistatic simulations diverges

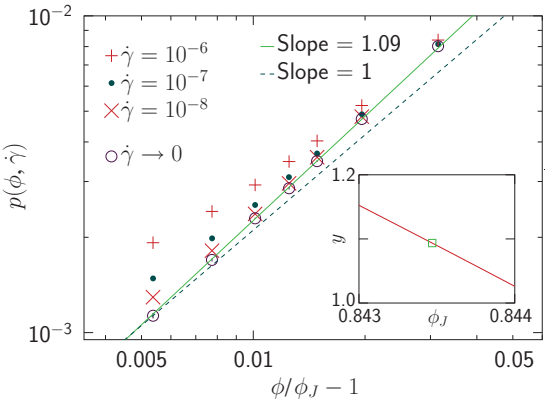

FIG. 5. (Color online) Alternative determination of the exponent y_p. The open circles are $p(\phi,\dot\gamma \to 0)$ from extrapolations of $p(\phi,\dot\gamma)$. Assuming $\phi_J = 0.843\,47$ the exponent becomes $y = 1.09$, shown by the solid line. The dashed line corresponds to $y = 1$. The inset shows how y depends on the assumed ϕ_J.

as ϕ_J is approached from above or from below. (This parallels the more rapid jumping between jammed and unjammed states reported in Ref. [12].) A dramatic change of the dynamical process that generates the ensemble suggests that the ensemble itself would depend on ϕ in a nontrivial way.

To conclude, we have shown that pressure and shear stress from shearing simulations are entirely consistent with the assumption of a critical behavior when corrections to scaling are included in the analysis. We find $\phi_J = 0.843\,47 \pm 0.000\,20$ and that, at ϕ_J, both p and σ scale as $\dot\gamma^q$ with $q = 0.28 \pm 0.02$. In the limit $\dot\gamma \to 0$ both p and σ vanish as $(\phi - \phi_J)^y$ with $y = 1.08 \pm 0.03$.

This work was supported by the Department of Energy Grant No. DE-FG02-06ER46298, the Swedish Research Council Grant No. 2007-5234, and a grant from the Swedish National Infrastructure for Computing (SNIC) for computations at HPC2N.

[1] A. J. Liu and S. R. Nagel, Nature (London) **396**, 21 (1998).
[2] C. S. O'Hern, L. E. Silbert, A. J. Liu, and S. R. Nagel, Phys. Rev. E **68**, 011306 (2003).
[3] P. Chaudhuri, L. Berthier, and S. Sastry, Phys. Rev. Lett. **104**, 165701 (2010).
[4] D. Vågberg, D. Valdez-Balderas, M. Moore, P. Olsson, and S. Teitel, (2010) e-print arXiv:1010.4752.
[5] P. Olsson and S. Teitel, Phys. Rev. Lett. **99**, 178001 (2007).
[6] T. Hatano, J. Phys. Soc. Jpn. **77**, 123002 (2008).
[7] T. Hatano, (2008) e-print arXiv:0804.0477.
[8] M. Otsuki and H. Hayakawa, Phys. Rev. E **80**, 011308 (2009).
[9] T. Hatano, Phys. Rev. E **79**, 050301 (2009).
[10] T. Hatano, Prog. Theor. Phys. Suppl. **184**, 143 (2010).
[11] B. P. Tighe, E. Woldhuis, J. J. C. Remmers, W. van Saarloos, and M. van Hecke, Phys. Rev. Lett. **105**, 088303 (2010).
[12] C. Heussinger and J.-L. Barrat, Phys. Rev. Lett. **102**, 218303 (2009).
[13] C. Heussinger, P. Chaudhuri, and J.-L. Barrat, Soft Matter **6**, 3050 (2010).
[14] D. J. Evans and G. P. Morriss, *Statistical Mechanics of Nonequilibrium Liquids* (Academic Press, London, 1990).
[15] D. J. Durian, Phys. Rev. Lett. **75**, 4780 (1995).
[16] K. Binder, Z. Phys. **43**, 119 (1981).
[17] T. S. Majmudar, M. Sperl, S. Luding, and R. P. Behringer, Phys. Rev. Lett. **98**, 058001 (2007).